Linearized Hybrid Stochastic/Robust Scheduling of Active Distribution Networks Encompassing PVs

Arash Baharvandi, Jamshid Aghaei, *Senior Member, IEEE*, Ahmad Nikoobakht, Taher Niknam, Vahid Vahidinasab, *Senior Member, IEEE, Damian Giaouris, Phil Taylor, Senior Member, IEEE,*

***Abstract*—This paper proposes an optimization framework to deal with the uncertainty in a day-ahead scheduling of smart active distribution networks (ADNs). The optimal scheduling for a power grid is obtained such that the operation costs of distributed generations (DGs) and the main grid are minimized. Unpredictable demand and PVs impose some challenges such as uncertainty. So, the uncertainty of demand and PVs forecasting errors are modeled using a hybrid stochastic/robust (HSR) optimization method. The proposed model is used for the optimal day-ahead scheduling of ADNs in a way to benefit from the advantages of both methods. Also, in this paper, the AC load flow constraints are linearized to moderate the complexity of the formulation. Accordingly, a mixed-integer linear programming (MILP) formulation is presented to solve the proposed day-ahead scheduling problem of ADNs. To evaluate the performance of the proposed linearized HSR (LHSR) method, the IEEE 33-bus distribution test system is used as a case study.**

***Index Terms*— Distributed Generations, Bounded Symmetric Optimization, Mixed Integer Linear Programming (MILP), Robust Optimization, Stochastic Optimization, Normal Distribution, Beta Distribution.**

NOMENCLATURE

The symbols used in this paper are listed and defined in this section.

A. Indices and Sets

i, Ψ_i	Index and Set of DGs, respectively.
t, Ψ_t	Index and Set of periods, respectively.
n, Ψ_n, N_b	Index and Set and total number of buses, respectively.
l, Ψ_l, N_l	Index and Set and total number of lines, respectively.
Ψ_i^n	Set of DGs placed at bus *n*.
D, Ψ_D^n	Index and set of demands placed at bus *n*.
$s(l)$	Sending bus of line *l*.
$r(l)$	Receiving bus of line *l*.

B. Parameters

C_t^{MG}	Locational marginal price of electricity at the substation bus at time *t* ($/MWh).
$p_{n,t}^D, q_{n,t}^D$	Forecasted active (MW) and reactive (MVAr) power of load at bus *n* in period *t*, respectively.
$S_{\max}^{MG}$	Maximum imported apparent power of main grid (MVA).
$S_{\max,i}^{DG}$	Maximum apparent power of DG *i* (MVA).
$S_{\max}^{l}$	Maximum apparent power flow of line *l* (MVA).
$V_{\min}$	Minimum voltage magnitude of buses (PU).
$V_{\max}$	Maximum voltage magnitude of buses (PU).
Y_l	Admittance of line *l* (PU).
G_l	Conductance of line *l* (PU).
β_l	Susceptance of line *l* (PU).
p_n^{PV}	Output power of PV placed at bus *n* (MW).

C. Variables

$p_{i,t}^{DG}, q_{i,t}^{DG}$	Generated active and reactive power by DG *i* in period *t*, respectively.
$p_{n,t}^{MG}, q_{n,t}^{MG}$	Injected active and reactive power by main grid to bus *n* in period *t*, respectively.
$V_{n,t}$	Magnitude of voltage of bus *n* in period *t* (PU).
$S_{l,t}$	Apparent power flow of line *l* in period *t* (MVA).
$p_{l,t}, q_{l,t}$	Active and reactive power flow of line *l* in period *t*.
$\alpha_{n,t}$	Voltage angle of bus *n* in period *t*.
φ	Angle between apparent power and active power.
C_i^{DG}	Cost function of DG *i* ($).

I. INTRODUCTION

A. Aims and Background

ACTIVE distribution network (ADN) is a new solution to realize wide and flexible access to various distributed generations (DGs), e.g., photovoltaics (PVs), in smart distribution systems. The widespread integration of renewable energy sources (RESs) and the increase of the number of PVs have brought new challenges to the safe and economic operation of the ADNs [1]. The main objective of the "active" network management is to coordinate the controllable DGs, PVs and demand loads.

In the traditional radial distribution networks, the power flow is unidirectional from generating station to the consumers. Nevertheless, the penetration of RESs has a significant impact on the power flow, voltage magnitude and reactive power flow in distribution networks. The AC load flow (AC-LF) model plays a vital role in the ADN to manage and realize the distributed power supply. Accordingly, the optimal day-ahead scheduling necessitates employing accurate

A. Baharvandi, J. Aghaei, and T. Niknam are with the Department of Electrical and Electronics Engineering, Shiraz University of Technology, Shiraz, Iran (e-mail: arash.baharvandi@gmail.com aghaei@sutech.ac.ir and niknam@sutech.ac.ir).
A. Nikoobakht is with the Higher Education Center of Eghlid, Eghlid, Iran- (email: a.nikoobakht@eghlid.ac.ir).
V. Vahidinasab is with the Abbaspour school of Engineering, Shahid Beheshti University, Tehran, Iran and School of Engineering, Newcastle University, Newcastle upon Tyne, UK (e-mail: v_vahidinasab@sbu.ac.ir, vahid.vahidinasab@newcastle.ac.uk).
D. Giaouris and P. Taylor are with the School of Engineering, Newcastle University, Newcastle upon Tyne, UK (e-mail: Damian.giaouris@newcastle.ac.uk, phil.taylor@newcastle.ac.uk).

AC-LF models. The AC-LF models can be formulated with different objective functions: minimization of energy costs, line congestion, voltage deviations or network losses [2]. Mathematically, the AC-LF models are inherently non-convex. Since, in the AC-LF models, there are both integer variables (representing resource statuses) and non-linear equations (AC-LF equations), they are in the form of mixed integer non-linear programming (MINLP).

Currently, the MINLP models are hard to solve and computationally intractable if they are directly solved by traditional MINLP solvers [3]. Accordingly, the economic operation of the ADN based on the AC-LF may not be a tractable problem even for the small size systems. Therefore, scheduling problems based on a linearized AC-LF model yield valid results near to nonlinear AC-LF, and it is more computationally efficient for the practical applications to have desirable solutions [4]. Although, the linearization of AC-LF model is not easy to obtain.

Furthermore, there are some uncertainties introduced by the loads and the presence of RESs as a result of forecasting errors in their day-ahead consumption/ production. This aspect makes the optimization problem even more complex as it includes uncertain parameters. Accordingly, the uncertainty modeling of RESs and loads can be developed by the available stochastic approach (SA) and/or robust approach (RA) [5] and [6]. Each method has its own 'pros and cons'. Some research works on the stochastic programming in the area have been reported in [7], [8] and [9]. A two-stage stochastic unit commitment model considering RESs is represented in [7] wherein the uncertain parameters are demand, wind, and PV. In order to account for the uncertainty around the true outcomes of load, wind, and PV, a minimum conditional value at risk term has been included in the formulation. In [8], a unit commitment problem with the stochastic solar power penetration is considered. In the first stage, the unit commitment, economic dispatch, and solar power scheduling decisions are formulated based on the day-ahead forecasted solar power and in the second stage, the solar power is planned and finally the uncertainty of solar power is discussed. The SA usually needs the generation of a rather large number of scenarios leading to large execution times, even for reasonably large values of the duality gap. Therefore, different scenario reduction approaches have been proposed to select the main scenarios while the small number of samples may lead to the infeasibility conditions. Stochastic programming is modeled while the expected total energy costs are minimized in [9] where in the first-stage of the stochastic model, the storage capacities (e.g., batteries) are determined. Run times and optimization gaps are significantly decreased by performing a dynamic cut selection procedure and a lower bound improvement plan within the stochastic dual dynamic programming framework. The SA usually needs the generation of a rather large number of scenarios leading to impossibly large executing times, even for reasonably large values of the duality gap [8]. Therefore, different scenario reduction approaches have been proposed to select the main scenarios that the small number of samples may lead to the infeasibility issues. That is, the day-ahead scheduling decision might not be feasible for some scenarios that are not selected. This is the main disadvantage of the SA. On the other hand, the RA has the advantages that the uncertainty is represented by a robust set instead of scenarios, and hence the problem remains a moderate complexity that does not grow with the number of scenarios and it requires minimal information of the input uncertain parameters. Similarly, the RA has been proposed to ensure the robustness and make the problem feasible for the most outcomes of the real time uncertain input parameters. Some research works have been focused on the RA in the area [6], [10] and [11]. In [6], the robust optimization model is presented for economic dispatch with wind power uncertainty under different levels of uncertainty budgets. In the ADNs, in order to address the uncertainties of the PV outputs, a two-stage RA is applied for the centralized optimal dispatch of PV inverters [10]. Similarly, a two-stage robust optimization model is presented for the uncertain wind power generation in [11] to harmonize the compensators of the discrete and continuous reactive power sources. However, while the objective function of the RA is to minimize the worst case cost, it always faces the challenges on over conservatism because the worst case scenario seldom occurs.

To address the above shortages of both stochastic and robust methods, in this paper, the SA and RA are combined to take advantages of the both stochastic and robust methods, particularly when the problem size is large and the historical data is not fully available.

B. Contributions

The main contributions of this paper are as follows.

− This paper presents an optimization framework for analyzing the PV integrated ADNs. The intrinsic uncertainties of the network in this problem are the uncertain loads and PV generations. Combination of the RA and SA are utilized to implement the uncertain parameters in the problem to benefit from both RA and SA features. Moreover, the output power of PVs is represented by Beta Probability Distribution Function (BPDF). Since, in the proposed hybrid stochastic/robust (HSR) approach, the uncertain parameter should have a normal PDF (NPDF), a new approximation methodology is introduced in a way to convert the BPDF to the NPDFs with the least possible error. That is, an NPDF with a specific mean and standard deviation replaces the BPDF that expresses the output power of the PVs. The previously mentioned NPDF which is above the curve of BPDF, has the lowest difference with the curve of BPDF when compared to any other NPDFs.

− In order to simplify the calculations, nonlinear load flow equations are approximated to piece-wisely linearized lines with specified slopes and intercept elevation which as compared to any other lines have the minimum difference with the nonlinear equations.

− The bounded and symmetric approach is utilized for uncertainty handling of the intermittent and uncertain PV power generation.

C. Structure of the paper

The rest of this paper is organized as follows. Section II describes the proposed method and states mathematical formulation. Section III provides the linearization of load flow. Section IV explains the PDF approximation. Simulation

Results and Discussion are presented in Section V. Finally, conclusions are drawn in Section VI.

II. Mathematical Formulation

In this section, the proposed methodology will be explained. The problem is formulated based on the proposed optimization framework wherein the operation cost function is minimized subject to the operation and technical constraints as expressed in the following subsections.

A. Proposed Methodology

In this section, the proposed method is proved. The problem based on combination robust optimization (RO) and stochastich programming (SP) is expressed as follows [13]:

$$\min/\max \quad q^T x + j^T y \tag{1}$$

$$Gx + Dy \le e \tag{2}$$

$$\sum_m g_{lm} x_m + \sum_i d_{li} y_i + \varepsilon\lambda \sqrt{\sum_{m\in M_l} g_{lm}{}^2 x_m{}^2 + \sum_{i\in I_l} d_{li}{}^2 y_i + e_l^2} \le e_l + \delta \max[1,|e_l|] \quad \forall l \tag{3}$$

$$\underline{x} \le x \le \bar{x} \tag{4}$$

$$y_i = 0,1 \qquad \forall i \tag{5}$$

$$g_{lm}^{true} = (1+\varepsilon\xi_{lm}) g_{lm} \tag{6}$$

$$d_{li}^{true} = (1+\varepsilon\xi_{li}) d_{li} \tag{7}$$

$$e_l^{true} = (1+\varepsilon\xi_l) e_l \tag{8}$$

In the above MILP problem, G and D are uncertain parameters. Also, x and y are variables. M_l and I_l are the set of indices regarding uncertain parameters. ξ is a variable related to the normal distribution. Constraints (6)-(8) denote the relation between true value and nominal value. In order to prove this problem, two conditions must be satisfied:

(i) the problem is feasible for the nominal value;

(ii) $\Pr\left\{\sum_m g_{lm}^{true} x_m + \sum_i d_{li}^{true} y_i > e_l^{true} + \delta \max[1,|e_l|]\right\} \le \kappa$

where $\lambda = F_n^{-1}(1-\kappa)$.

Proof of condition (ii):

$$\Pr\left\{\sum_m g_{lm}^{true} x_m + \sum_i d_{li}^{true} y_i > e_l^{true} + \delta \max[1,|e_l|]\right\}$$

$$= \Pr\left\{\begin{array}{l} \sum_m g_{lm} x_m + \varepsilon \sum_{m\in M_l} \xi_{lm} |g_{lm}| x_m \\ + \sum_i d_{li} y_i + \varepsilon \sum_{i\in I_l} \xi_{li} |d_{li}| y_i > \\ e_l + \varepsilon\xi_l |e_l| + \delta \max[1,|e_l|] \end{array}\right\}$$

$$\le \Pr\left\{\underbrace{\frac{\sum_{m\in M_l} \xi_{lm} |g_{lm}| x_m + \sum_{i\in I_l} \xi_{li} |d_{li}| y_i - \xi_l |e_l|}{\sqrt{\sum_{m\in M_l} g_{lm}{}^2 x_m{}^2 + \sum_{i\in I_l} d_{li}{}^2 y_i + e_l^2}}}_{=\Lambda} > \lambda\right\}$$

$$= 1 - \Pr\{\Lambda \le \lambda\} = 1 - F_n(\lambda) = 1 - (1-\kappa) = \kappa$$

Where, Λ is a random variable with standardized normal distribution. Also, if the non-equality constraint (2) is converted to the equality constraint, then:

$$Gx + Dy \ge e \tag{9}$$

$$\sum_m g_{lm} x_m + \sum_i d_{li} y_i + \varepsilon\lambda \sqrt{\sum_{m\in M_l} g_{lm}{}^2 x_m{}^2 + \sum_{i\in I_l} d_{li}{}^2 y_i + e_l^2} \le e_l + \delta \max[1,|e_l|] \quad \forall l \tag{10}$$

B. Problem Statement

The objective function of the problem is defined as follows:

$$\min f(y,u) = \sum_{T\in\Psi_t} \left(\sum_{i\in\Psi_i} C_i^{DG} p_{i,t}^{DG} + \sum_{n\in\Psi_n} C_t^{MG} p_{n,t}^{MG} \right) \tag{11}$$

$$y = [p_{i,t}^{DG}, p_{n,t}^{MG}] \tag{12}$$

$$u = [V_{n,t}, S_{l,t}] \tag{13}$$

$$V_{n,t} = [V_{1,t}, V_{2,t}, ..., V_{N_b,t}] \tag{14}$$

$$S_{l,t} = [S_{1,t}, S_{2,t}, ..., S_{N_l,t}] \tag{15}$$

In (11), the first term and second term are related to the operation cost of DGs and the cost of injected power by the main grid, respectively. The vector of y is introduced as control variables in (12) and u states the dependent variables in (13). In (4) and (5), the components of these vectors are represented.

Quadratic cost function of a DG is described as follow [21]:

$$C_i^{DG}(p_{i,t}^{DG}) = a_i + b_i p_{i,t}^{DG} + c_i (p_{i,t}^{DG})^2 \tag{16}$$

In addition, it should be noted that the operation cost of the reactive power of the DGs and the main grid has been ignored. The operation constraints on this problem based on the combination of robust and stochastic methods are discussed below [12], [13]:

$$p_{n,t}^{MG} + \sum_{i\in\Psi_i^n} p_{i,t}^{DG} - \sum_{l:s(l)=n} p_{l,t}(V_{s(l),t}, V_{r(l),t}, Y_l, \alpha_{s(l),r(l)}) + \sum_{l:r(l)=n} p_{l,t}(V_{s(l),t}, V_{r(l),t}, Y_l, \alpha_{s(l),r(l)}) \ge \sum_{D\in\Psi_D^n} p_{n,t}^D \quad \forall n, \forall t \tag{17}$$

$$p_{n,t}^{MG} + \sum_{i\in\Psi_i^n} p_{i,t}^{DG} - \sum_{l:s(l)=n} p_{l,t}(V_{s(l),t}, V_{r(l),t}, Y_l, \alpha_{s(l),r(l)}) + \sum_{l:r(l)=n} p_{l,t}(V_{s(l),t}, V_{r(l),t}, Y_l, \alpha_{s(l),r(l)}) \le \sum_{D\in\Psi_D^n} p_{n,t}^D + \delta \max\left\{1, \left|\sum_{D\in\Psi_D^n} p_{n,t}^D\right|\right\} - \varepsilon\lambda \sum_{D\in\Psi_D^n} p_{n,t}^D \quad \forall n, \forall t \tag{18}$$

$$q_{n,t}^{MG} + \sum_{i\in\Psi_i^n} q_{i,t}^{DG} - \sum_{l:s(l)=n} q_{l,t}(V_{s(l),t}, V_{r(l),t}, Y_l, \alpha_{s(l),r(l)}) + \sum_{l:r(l)=n} q_{l,t}(V_{s(l),t}, V_{r(l),t}, Y_l, \alpha_{s(l),r(l)}) \ge \sum_{D\in\Psi_D^n} q_{n,t}^D \quad \forall n, \forall t \tag{19}$$

$$q_{n,t}^{MG}+\sum_{i\in\Psi_i^n}q_{i,t}^{DG}-\sum_{l:s(l)=n}q_{l,t}(V_{s(l),t},V_{r(l),t},Y_l,\alpha_{s(l),r(l)})$$
$$+\sum_{l:r(l)=n}q_{l,t}(V_{s(l),t},V_{r(l),t},Y_l,\alpha_{s(l),r(l)})\le\sum_{D\in\Psi_D^n}q_{n,t}^{D}$$
$$+\delta\max\left\{1,\left|\sum_{D\in\Psi_D^n}q_{n,t}^{D}\right|\right\}-\varepsilon\lambda\sum_{D\in\Psi_D^n}q_{n,t}^{D}\qquad\forall n,\forall t \tag{20}$$

$$\max\left\{1,\left|\sum_{D\in\Psi_D^n}p_{n,t}^{D}\right|\right\}=\sum_{D\in\Psi_D^n}p_{n,t}^{D}z_1+z_2\qquad\forall n,\forall t \tag{21}$$

$$\max\left\{1,\left|\sum_{D\in\Psi_D^n}q_{n,t}^{D}\right|\right\}=\sum_{D\in\Psi_D^n}q_{n,t}^{D}z_3+z_4\qquad\forall n,\forall t \tag{22}$$

$$z_1+z_2=1 \tag{23}$$

$$z_3+z_4=1 \tag{24}$$

$$\sum_{D\in\Psi_D^n}p_{n,t}^{D}z_1\ge z_1\qquad\forall n,\forall t \tag{25}$$

$$\sum_{D\in\Psi_D^n}p_{n,t}^{D}z_2\le z_2\qquad\forall n,\forall t \tag{26}$$

$$\sum_{D\in\Psi_D^n}q_{n,t}^{D}z_3\ge z_3\qquad\forall n,\forall t \tag{27}$$

$$\sum_{D\in\Psi_D^n}q_{n,t}^{D}z_4\le z_4\qquad\forall n,\forall t \tag{28}$$

Constraints (17) and (19) are related to active and reactive power balance in the grid, respectively, that are relaxed. Constraints (18), (20) are the same as (17) and (19), where uncertainty is also considered in them and δ represents the infeasibility tolerance. Besides, ε and κ are defined as uncertainty and reliability level, respectively. In this method, a constraint that has an uncertain parameter should be displayed as (18) and (20). Here, the load demand, as an uncertain parameter, is written in three terms in the right-hand side of equation (18). Moreover, κ is a function of λ which is shown as follows:

$$\kappa=1-\int_{-\infty}^{\lambda}\frac{1}{\sqrt{2\pi}}\exp(-\frac{x^2}{2})dx \tag{29}$$

It is noted that we have $\delta\ge\varepsilon\lambda$, otherwise, the problem would be infeasible. Constraints (21) and (22) correspond to the second term of the right side of the constraints (18) and (20). Indeed, the multiplied term by δ in constraints (18) and (20) is nonlinear. To linearize these terms, the right side of constraints (21) and (22) should be replaced for them to be used in the constraints (23)-(28). Constraint (23) states that only one of the binary variables z_1, z_2 can be equal to 1. Constraint (24) is similar to constraint (23). In (25), if $z_1=1$, $p_{n.t}^{D}\ge 1$, according to (23), $z_2=0$ and the maximum of 1 and $p_{n.t}^{D}$ is equal to $p_{n.t}^{D}$ corresponding to the right side of constraint (11). In (26), if $z_2=1$, then $p_{n.t}^{D}\le 1$, and according to (23), $z_1=0$ and maximum of 1 and $p_{n.t}^{D}$ is equal to 1 that it corresponds to the right side of constraint (21). In (27), if $z_3=1$, we have $q_{n.t}^{D}\ge 1$, according to (24), $z_4=0$ and the maximum of 1 and $q_{n.t}^{D}$ is equal to $q_{n.t}^{D}$ that it corresponds to the right side of constraint (22). In (28), if $z_4=1$, $q_{n.t}^{D}\le 1$, according to (24), $z_3=0$ and maximum of 1 and $q_{n.t}^{D}$ is equal to 1 that it corresponds to the right side of constraint (22). Constraints of DG, the main grid and power grid are represented as follows:

$$(p_{n,t}^{MG})^2+(q_{n,t}^{MG})^2\le(S_{\max}^{MG})^2\qquad\forall n,\forall t \tag{30}$$

$$(p_{i,t}^{DG})^2+(q_{i,t}^{DG})^2\le(S_{\max,i}^{DG})^2\qquad\forall i,\forall t \tag{31}$$

$$(p_{l,t})^2+(q_{l,t})^2\le(S_{\max}^{l})^2\qquad\forall l,\forall t \tag{32}$$

$$V_{\min}\le V_{n,t}\le V_{\max}\qquad\forall n,\forall t \tag{33}$$

Constraint (30) certifies that the imported active and reactive power by the main grid is restricted to the maximum apparent power of transformer. Constraint (31) keeps the ratings of generated active and reactive power by DGs. Also, in (32), the range of active and reactive power flow in the branches is taken into account. Upper and lower limits of voltage are indicated in (33). Also, it should be noted that when the PV is connected to the network, the active power load ($p_{n.t}^{D}$) is replaced by the new variable named net load ($p_{n.t}^{Net}$) as follows:

$$p_{n,t}^{Net}=\sum_{D\in\Psi_D^n}p_{n,t}^{D}-p_n^{PV}\qquad\forall n,\forall t \tag{34}$$

$max\{1.|p_{n.t}^{Net}|\}$ in (21) is determined by the size of PV. Thus, if the difference between load and output power of the PV is greater than one, then the constraint (21) is equal to the net load, otherwise, it equals one.

C. Deterministic Problem

If the uncertainties of the network are not considered, the problem changes to the deterministic form. The deterministic problem is the same as the previous subsection, with the difference that constraints (35) and (36) replace the constraints (17)-(29).

$$p_{n,t}^{MG}+\sum_{i\in\Psi_i^n}p_{i,t}^{DG}-\sum_{l:s(l)=n}p_{l,t}(V_{s(l),t},V_{r(l),t},Y_l,\alpha_{s(l),r(l)})$$
$$+\sum_{l:r(l)=n}p_{l,t}(V_{s(l),t},V_{r(l),t},Y_l,\alpha_{s(l),r(l)})=\sum_{D\in\Psi_D^n}p_{n,t}^{D}\qquad\forall n,\forall t \tag{35}$$

$$q_{n,t}^{MG}+\sum_{i\in\Psi_i^n}q_{i,t}^{DG}-\sum_{l:s(l)=n}q_{l,t}(V_{s(l),t},V_{r(l),t},Y_l,\alpha_{s(l),r(l)})$$
$$+\sum_{l:r(l)=n}q_{l,t}(V_{s(l),t},V_{r(l),t},Y_l,\alpha_{s(l),r(l)})=\sum_{D\in\Psi_D^n}q_{n,t}^{D}\qquad\forall n,\forall t \tag{36}$$

The constraints (35) and (36) are equivalent to active and reactive power equations in the network, respectively, wherein the uncertainty is not considered.

III. Linearization of Load Flow

To facilitate the problem solving, the nonlinear equations of load flow are linearized. In [14], a linearized load flow for the practical implementation has been applied. AC feasibility, the ability to handle large-scale real power systems and lower computational complexity are the main features of the linearized AC network [15]. These nonlinear equations are as follows:

$$p_{l,t}=G_lV_{s(l)}^2-G_lV_{s(l)}V_{r(l)}\cos(\alpha_{s(l),t}-\alpha_{r(l),t})$$
$$+\beta_lV_{s(l)}V_{r(l)}\sin(\alpha_{s(l),t}-\alpha_{r(l),t})\qquad\forall l,\forall t \tag{37}$$

$$q_{l,t} = \beta_l V_{s(l)}^2 - \beta_l V_{s(l)} V_{r(l)} \cos(\alpha_{s(l),t} - \alpha_{r(l),t}) - G_l V_{s(l)} V_{r(l)} \sin(\alpha_{s(l),t} - \alpha_{r(l),t}) \quad \forall l, \forall t \quad (38)$$

In Eqs. (37) and (38), active and reactive power flow of lines are represented, respectively. In order to linearize these equations, the following activities are performed:

$$V_{n,t} = 1 + \Delta V_{n,t} \quad \forall n, \forall t \quad (39)$$

$$p_{l,t} = G_l(1 + 2\Delta V_{s(l),t}) - G_l(1 + \Delta V_{s(l),t} + \Delta V_{r(l),t})\cos(\alpha_{s(l),t} - \alpha_{r(l),t}) + \beta_l(1 + \Delta V_{s(l),t} + \Delta V_{r(l),t})\sin(\alpha_{s(l),t} - \alpha_{r(l),t}) \quad (40)$$

$$q_{l,t} = B_l(1 + 2\Delta V_{s(l),t}) - \beta_l(1 + \Delta V_{s(l),t} + \Delta V_{r(l),t})\cos(\alpha_{s(l),t} - \alpha_{r(l),t}) - G_l(1 + \Delta V_{s(l),t} + \Delta V_{r(l),t})\sin(\alpha_{s(l),t} - \alpha_{r(l),t}) \quad (41)$$

In (39), the voltage magnitude has been written in terms of voltage variations. By replacing (39) in (37) and (38) and using Teylor extension, the equations (40) and (41) are obtained. Then, a mathematical approximation is used as follows:

$$\Delta V_{s(l),t} + \Delta V_{r(l),t} \cong \sin(\Delta V_{s(l),t} + \Delta V_{r(l),t}) \quad (42)$$

Since the voltage variation is close to zero, it can be approximated by the *sinus* of these changes, as seen in (42). By locating (42) in (40) and (41), equations (43) and (44) are attained:

$$p_{l,t} = G_l + 2G_l\Delta V_{s(l),t} - G_l\cos(\gamma_{l,t}) - G_l(\sin(\theta_{l,t}) - \sin(\gamma_{l,t})) + \beta_l\sin(\gamma_{l,t}) + \beta_l(\cos(\gamma_{l,t}) - \cos(\theta_{l,t})) \quad (43)$$

$$q_{l,t} = \beta_l + 2\beta_l\Delta V_{s(l),t} - \beta_l\cos(\gamma_{l,t}) - \beta_l(\sin(\theta_{l,t}) - \sin(\gamma_{l,t})) - G_l\sin(\gamma_{l,t}) - G_l(\cos(\gamma_{l,t}) - \cos(\theta_{l,t})) \quad (44)$$

$$\alpha_{s(l),t} - \alpha_{r(l),t} = \gamma_{l,t} \quad (45)$$

$$\Delta V_{s(l),t} + \Delta V_{r(l),t} + \alpha_{s(l),t} - \alpha_{r(l),t} = \theta_{l,t} \quad (46)$$

In deriving equations (43) and (44), the trigonometric relations (multiplication to sum) are utilized. Eqs. (45) and (46) are used to express the equations (43) and (44).

A. *Linearization of* sin *(x)*

If the trigonometric functions can be approximated in equations (43) and (44) with an *innovative optimal piece-wise linearization technique*, the load flow equations become linear. To this end, to linearize the sin *(x)*:

$$f(x) = |\sin x - (m_1 x + e_1)| \quad (47)$$

In (47), first, for a specified m_1, e_1 and $-1 \le x \le 1$, $f(x)$ values are distinguished. Then, the maximum value is determined. In the following, for the other specified m_1, e_1 and $-1 \le x \le 1$, $f(x)$ values are determined and again the maximum value is assigned. This procedure will continue for different lines. Finally, the minimum value is chosen among the maximum values. This minimum value corresponds to the best alternative line of the *sinus* function. In Fig. 1(a), the line that is the best approximation for sin *(x)* has m_1= 0.9, e_1= 0. In this case, the maximum value of *f(x)* is 0.0585 which is less than the maximum value of *f(x)* for any other lines.

B. *Linearization of* cos *(x)*

For approximating *cos(x)* by a linear function, (*mx+e*), the following approximation formulations can be adopted:

$$g(x) = |\cos x - (mx + e)| \quad (48)$$

$$\cos x \cong (m_2 x + e_2)w_1 + (m_3 x + e_3)w_2 = \Omega_1 + \Omega_2 \quad (49)$$

$$w_1 + w_2 = 1 \quad (50)$$

$$\Omega_1 \ge -w_1 K_1 \quad (51)$$

$$\Omega_1 \le w_1 K_2 \quad (52)$$

$$\Omega_1 \ge (m_2 x + e_2) - (1 - w_1)K_3 \quad (53)$$

$$\Omega_1 \le (m_2 x + e_2) + (1 - w_1)K_4 \quad (54)$$

$$\Omega_2 \ge -w_2 K_5 \quad (55)$$

$$\Omega_2 \le w_2 K_6 \quad (56)$$

$$\Omega_2 \ge (m_3 x + e_3) - (1 - w_2)K_7 \quad (57)$$

$$\Omega_2 \le (m_3 x + e_3) + (1 - w_2)K_8 \quad (58)$$

Eq. (48) is similar to (47). In the interval -1 to 1, cos *(x)* should be approximated by two lines, which is shown in (49). Due to the multiplication of binary variables (w_1, w_2) in another variable, equation (49) is nonlinear. To deal with this nonlinearity, the first and second terms in the equation (49) are equal to Ω_1 and Ω_2 and are exerted from constraints (50) to (58). In (50), it is represented that only one of the binary variables w_1 and w_2 can be equal to 1. In (41) and (52), if w_1=1, then $\Omega_1 \ge -K_1$, $\Omega_1 \le K_2$ that $K_1 = -0.6$, $K_2 = 1$ and according to (53) and (54), $\Omega_1 = m_2 x + e_2$ and since w_2 = 1, according to (55) and (56), $\Omega_2 = 0$ and constraints (57) and (58) are inactive wherein K_7 and K_8 are big numbers. In (55) and (56), if w_2 = 1, then $\Omega_2 \ge -K_5$, $\Omega_2 \le K_6$ that K_5 =-0.6, $K_6 = 1$ and according to (57) and (58), $\Omega_2 = m_3 x + e_3$ and while w_1 = 1, according to (51) and (52), $\Omega_1 = 0$ and constraints (53) and (54) are inactive in which K_3 and K_4 are large numbers.

Fig. 1(b) shows two lines that are the best approximation for cos*(x)* which have m_2=0.4, $e_2 = 1$, m_3=-0.4, $e_3 = 1$. The maximum difference between two lines with cos *(x)* is 0.0811 which is less than the maximum difference of any other possible lines. In order to linearize the constraints (30)-(32), the following constraints can be applied:

$$p \le S_{\max}\cos\varphi \quad (59)$$

$$p \le S_{\max}(m\varphi + e) \quad (60)$$

Constraint (59) is the same nonlinear constraint, which is linearized with the procedure described above for cos *(x)* as shown in (60). Accordingly, by implementing the proposed linearization technique, the day-ahead scheduling problem of active distribution networks is converted to an MILP model.

IV. PDF Approximation

To deal with the uncertainties (load and PV generation uncertainties) of the day-ahead scheduling of ADNs, a combination of RA and SA have been adopted. In the proposed method, the uncertain parameter should be modeled by a NPDF.

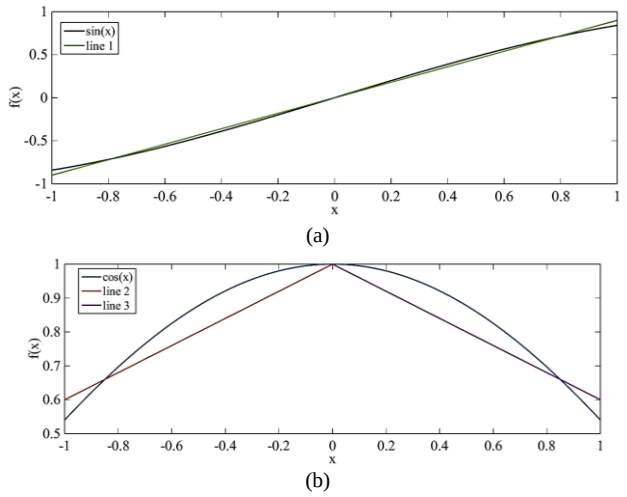

Fig. 1. Approximation of trigonometric functions to linear functions. (a) sin *(x)*. (b) cos *(x)*

Normally, the load is expressed by the NPDF, but the PV power is characterized by the Beta PDF [16]. In the previous section, the difference between load and PV output power is defined as the *net load*. Since, the net load is the uncertain parameter, it should be expressed by an NPDF. Therefore, if one can approximate the Beta PDF of the PV to the Normal PDF, then the net load is an uncertain parameter which is described by the normal PDF, and the proposed method can be used (which is a uncertain parameter to be described by a normal PDF). According to the technique proposed here, the BPDF of the PV generated power can be approximated by NPDF. The BPDF is represented as [17]:

$$f(x)=\frac{x^{\tau-1}(1-x)^{\vartheta-1}}{B(\tau,\vartheta)} \tag{61}$$

$$B(\tau,\vartheta)=\frac{\Gamma(\tau)\Gamma(\vartheta)}{\Gamma(\tau+\vartheta)} \tag{62}$$

In (61) and (62), τ and ϑ are two positive shape parameters and Γ is gamma function. Approximation of BPDF to NPDF is carried out as follows:

$$ID(p_{PV})=\left|\begin{array}{l}\int_{\rho_1}^{\rho_2}\frac{p_{PV}{}^{\tau-1}(1-p_{PV})^{\vartheta-1}}{B(\tau,\vartheta)}dp_{PV}\\ -\int_{\rho_1}^{\rho_2}\frac{1}{\sqrt{2\pi}\sigma}\exp\left(-0.5(\frac{p_{PV}-\mu}{\sigma})^2\right)dp_{PV}\end{array}\right| \tag{63}$$

In (63), *ID* (p_{PV}) is the integral difference between BPDF and NPDF. First and second integrals are related to BPDF and NPDF, respectively. Since the surface below the distribution function in an interval is equal to the probability of a variable in the same interval, if for an NPDF, it is found that the area under curve has the minimum difference with the surface below BPDF, this NPDF can be considered as the best approximation for the BPDF. In other words, different NPDFs are placed in (63) and each time the integral difference is determined. Among the integral differences, the minimum integral difference is specified as the best NPDF to approximate the BPDF. If τ = 4.2 and ϑ=1.8 [18], ρ_1 = 0.5 and ρ_2 = 0.9, then the approximation of BPDF to NPDF is seen in Fig. 2. The minimum integral difference pertains to NPDF with μ=0.7 and σ=0.2 and the value of the minimum is 0.056. Thus, with this approximation, the above-mentioned approach can be utilized. The percent error of the average approximated distribution is 4.76%, which is acceptable.

V. Simulation Results and Discussion

In this section, all simulations are utilized to appraise the proposed approach. The case studies are executed using CPLEX solver within GAMS [19] on a personal computer with Core i7 processor and 8 GB RAM.

A. IEEE 33-bus Distribution Test System

In Fig. 3, the single line diagram of the IEEE 33-bus 12.66 kV and 5 MVA radial distribution network is illustrated. All of the data in this network and load profile are detected in [20] and [21]. Maximum apparent power flow in the lines 1-9 and 10-32 is 6 MVA and 3 MVA, respectively. Also, it is assumed the maximum imported apparent power from the main grid to the grid is infinite.

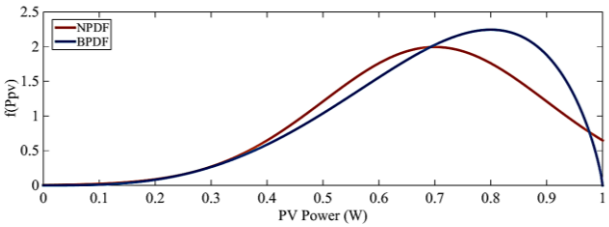

Fig. 2. Approximation of BPDF by NPDF.

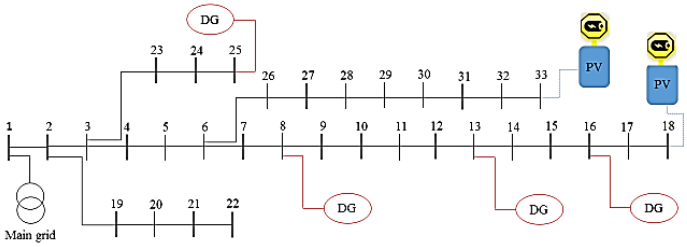

Fig. 3. The IEEE 33-bus radial distribution test system [20]

This network is equipped with 4 diesel-based DGs at buses 8, 13, 16 and 25. The cost coefficients and technical data of DGs are shown in Table II. The data of the forecasted day-ahead active and reactive load and day-ahead wholesale electricity prices can be found in [20]. Load ratios for all buses is considered to be equal.

1) *Case I: Uncertain modeling by the proposed LHSR method:* Here, the uncertain parameter is the net load and problem formulation is related to subsection B of the section II. The results of the hourly cost in the LHSR are represented in Table III. As it can be seen, with the increasing of the load, especially during peak hours, the cost of operation increases. Additionally, the wholesale electricity prices are higher at the peak hours. Also, the range of voltage magnitude is 0.95 to 1.05 pu. PVs can be integrated into the network. The output power of PV is considered as an uncertain parameter and is described by the BPDF, which is approximated to the NPDF as described in section IV. Accordingly, the difference between load and PV power is defined as the net load, see Eq. (34), which is considered as the uncertain parameter. In Fig. 3, two PVs are placed on buses 18 and 33, as the forecasted

output power of the both PVs is 1 MW for day hours [22]. In the all results it is assumed that the PV has storage (see Fig. 3) and produces 1 MW in each hour even at night. As it can be observed in Table III, the PV reduces the hourly and total costs. The total cost of the case without PV is 62357.124$, while its value in the case with PV is 58840.04$ and accordingly, the cost reduction is equal to 3517.084$. By integrating the PVs into the network, the injected power through the main grid as well as the generated power by DGs are reduced, which reduces the cost.

TABLE II: Cost coefficients and technical data for DG units

Unit	Cost function coefficients			Technical constraints	
	a_i ($)	b_i ($/MW)	c_i ($/MW^2)	S_{min}^{DG}	S_{max}^{DG}
DG1	27	79	0.0035	1	4.12
DG2	25	87	0.0045	1	3.53
DG3	28	92	0.0045	1	3.53
DG4	29	81	0.0035	1	4.83

TABLE III: Hourly and total cost results for linearized problem (case I)

hour	Operation cost ($) (no PV)	Operation cost ($) (with PV)	Cost reduction($)
1	1626.704	1540.919	85.785
2	1461.966	1382.166	79.800
3	1347.632	1273.817	73.815
4	1262.838	1193.013	69.825
5	1192.737	1128.897	63.840
6	1372.028	1296.218	75.810
7	1482.539	1402.739	79.800
8	1841.998	1744.243	97.755
9	1977.711	1875.966	101.745
10	2280.569	2161.868	118.701
11	2665.962	2522.970	142.992
12	2834.142	2680.979	153.168
13	3347.768	3159.038	188.73
14	3889.931	3661.042	228.889
15	4471.128	4199.188	271.94
16	4553.418	4275.104	278.314
17	4514.452	4237.405	277.047
18	4341.492	4075.897	265.595
19	3607.794	3398.804	208.990
20	2923.465	2763.894	159.571
21	2683.026	2538.684	144.342
22	2597.046	2457.880	139.166
23	2217.915	2102.205	115.710
24	1862.864	1767.104	95.760
Total	62357.124	58840.040	3517.084

This is shown in Figs. 4, 5 and 6 (i.e. the linearized and nonlinear problem). In the first 12 hours of the day, due to lower demand and cost of the main grid, the DGs produce 1 MW, which is the minimum output power of DGs and the grid is supplied by the main grid. From 13:00 to 19:00, due to the increased demand of power grid, the production capacity of DGs should exceed their minimum capacity to achieve the optimal cost. From 20:00 to 24:00, DGs production are the same as in the first 12 hours. As it can be seen from these figures, the output power of DGs and the imported power of the main grid in the no PV case is greater than the PV–integrated case, which shows the impact of the PVs. Fig. 7 represents the output power of DGs for the nonlinear problem. According to this figure, it is possible to compare the output power of DGs of both linear and nonlinear cases and obtain the error of load flow linearization. For example, the power output of the DG1 at 14 o'clock are 3.185 and 3.121 for linear and nonlinear load flows, respectively. The error rate for the linearization is about 2% for the output power showing a negligible linearization error for the load flow. It should be noted that the values of ε, λ and δ in both cases are 0.05. This value indicates that the results obtained by the simulations have 5% uncertainty. As ε increases, the total cost increases and subsequently the uncertainty of the results is augmented. Fig. 8 represents the total cost of the case I with PV under different values of ε and κ and δ=0.05. For κ >0.5 that λ<0, according to (29), the total cost is more than the case κ <0.5 that λ>0. Because of λ<0, the right side of Eq. (18) increases and this is similar to increasing the load leading to an increase in the cost. The cost is generally reduced with the increase of λ and ε. The small tale in the Fig. 8 states that by decreasing the κ and keeping the ε constant, the value of the objective function is reduced. The results of the nonlinear problem (NLP), (11)-(34) and (37)-(38), are shown in Table IV. The total cost in the nonlinear problem for the no PV and with PV are $61219.837 and 57701.732, respectively. The difference between the results of the linear and nonlinear problems is low. The time duration of the simulation is represented in Table V. For instance, the duration of times in case I (no PV) for the both linear and nonlinear problems are 125 and 1307 seconds, respectively. The error percentages of the linearized problem for no PV and with PV are 1.8% and 1.93%, respectively.

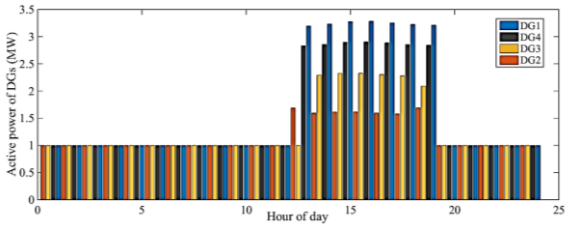

Fig. 4. Optimal generated active power by DGs (case I&no PV&linear)

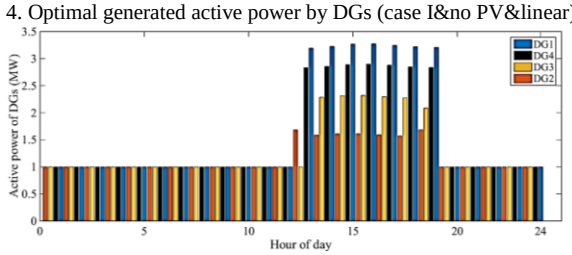

Fig. 5. Optimal generated active power by DGs (case I&with PV&linear)

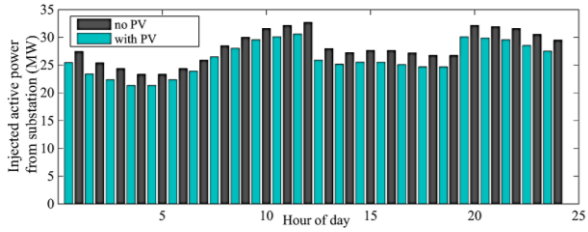

Fig. 6. Injected active power by main grid (case I)

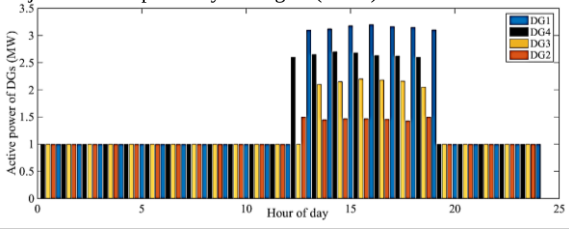

Fig. 7. Optimal generated active power by DGs (case I&no PV&nonlinear)

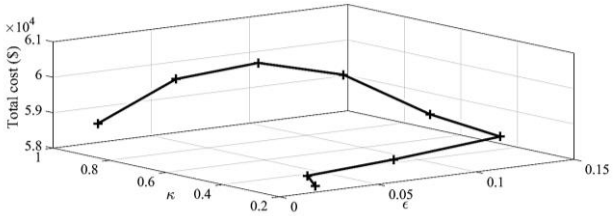

Fig. 8. Total cost of case I, LP-with PV, under different values of ε and κ

TABLE IV: Hourly and total cost results for nonlinear problem (case I)

Hour	Operation cost ($) (no PV)	Operation cost ($) (PV integrated)	Cost reduction ($)
1	1626.704	1540.919	85.785
2	1461.966	1382.166	79.800
3	1347.632	1273.817	73.815
4	1262.838	1193.013	69.825
5	1192.738	1128.897	63.841
6	1372.028	1296.218	75.810
7	1482.539	1402.739	79.800
8	1841.998	1744.243	97.755
9	1977.711	1875.966	101.745
10	2280.569	2159.059	121.510
11	2665.962	2521.407	144.555
12	2834.142	2681.207	152.935
13	3320.590	3132.040	188.550
14	3769.371	3543.111	226.260
15	4254.429	3988.364	266.065
16	4321.877	4049.527	272.350
17	4274.422	3999.977	274.445
18	4118.745	3852.680	266.065
19	3529.260	3319.760	209.500
20	2923.465	2762.150	161.315
21	2683.026	2536.376	146.650
22	2597.046	2445.586	151.46
23	2217.915	2096.405	121.510
24	1862.864	1767.104	95.760
Total	61219.837	57701.732	3518.105

TABLE V: Time duration of simulation (case I)

Type of problem	Linearized problem (no PV)	Linearized problem (PV included)	Nonlinear problem (no PV)	Nonlinear problem (PV included)
Computation time (s)	125	136	1307	1324

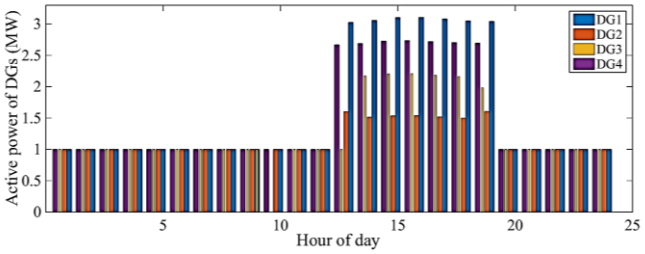

Fig. 9. Optimal generated active power by DGs for linearized problem (case II)

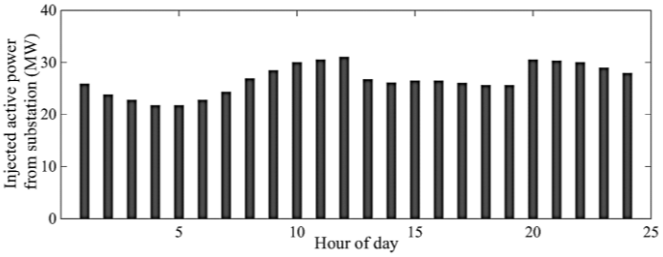

Fig. 10. Injected active power by main grid for linearized problem (case II)

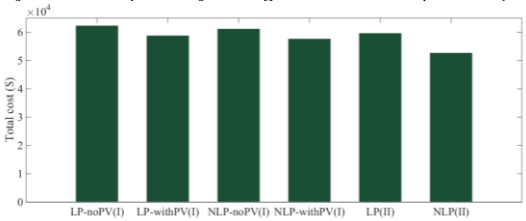

Fig. 11. Total costs of both cases in different states

2) *Case* II: *Deterministic Problem*: In this case, the formulation of the subsection C of the section II is used while the uncertainty modeling is ignored. Also, PVs are not included in this case. The results of the simulation for the linearized and nonlinear problem are represented in Table VI. As seen, the total cost in LP is 59684.715 ($) and in NLP is 52738.525 ($). The output power of DGs and the power input to the network through the main grid for the linearized problem are shown in Figs. 9 and 10, respectively. As in the previous case, DG power has been increased during peak hours, resulting in fewer injections to the network through the main grid, and during the rest of the time, DG power is lowered and injected power is increased by the main grid. In Fig. 11, the total cost of both cases for different states is illustrated where the total cost of the deterministic problem is less than the case I while the uncertainty has been ignored. The simulation execution times are represented in Table VII. This time for the NLP is 1061 seconds. It is clear that because of intrinsic complexity of the NLP, it takes a long time for the model to respond as the dimension enlarges.

TABLE VI: Hourly and total costs (case II)

Hour	Operation cost ($) (linearized problem)	Operation cost ($) (nonlinear problem)	Difference ($)
1	1558.969	1558.969	0
2	1398.750	1398.750	0
3	1289.063	1289.063	0

4	1207.344	1207.344	0
5	1142.000	1142.000	0
6	1311.875	1311.875	0
7	1419.375	1419.375	0
8	1764.938	1764.938	0
9	1897.703	1897.703	0
10	2186.813	2186.813	0
11	2552.734	2552.734	0
12	2712.563	2712.563	0
13	3201.505	2898.938	302.567
14	3720.458	2939.672	780.786
15	4276.783	2980.406	1296.377
16	4355.548	2980.406	1375.142
17	4318.408	2939.672	1378.736
18	4152.203	2898.938	1253.265
19	3450.108	2890.791	559.702
20	2797.109	2797.109	0
21	2568.844	2568.844	0
22	2487.125	2487.125	0
23	2127.000	2127.000	0
24	1787.500	1787.500	0
Total	59684.715	52738.525	6946.19

TABLE VII: Time duration of simulation (case II)

Type of problem	Linearized problem	Nonlinear problem
Duration time (seconds)	134	1061

These problems belong to the NP-hard category, and the solution time increases exponentially as the problem size rises, in other words. However, by applying the proposed linearized formulation the execution time has been significantly decreased to 134 Seconds which implies the advantage of the linearization. Since the uncertain parameter in the uncertainty model is slightly more than its nominal value, the difference in linear and nonlinear results in the uncertain model is less than the results in the deterministic model. Indeed, the uncertain parameter in the active power balance equation causes the variables to be closer together than deterministic model in the linear and nonlinear problems to achieve the optimal solution.

B. IEEE 69-bus Distribution Test System

All data of IEEE 69-bus and load profile are given in [23], [24].

Case I*: Uncertain modeling by the proposed LHSR method:* In this case, there are uncertain parameters of the PV power and the load. Three PVs are located on buses 8, 33 and 61. Their predicted output powers are 0.5 kW. The simulation results for the linearized problem are presented in Table VIII. As seen in Table VIII, the PV reduces the hourly and total costs. The total costs of the case I (linearized problem) without and with PV are 18885.940$ and 17252.621$, respectively.

TABLE VIII: Hourly and total cost results for linearized problem (case I)

hour	Operation cost ($) (no PV)	Operation cost ($) (with PV)	Cost reduction($)
1	541.449	477.110	64.339
2	526.740	466.890	59.850
3	516.919	461.557	55.362
4	513.031	460.663	52.368
5	510.392	462.512	47.880
6	526.444	469.586	56.858
7	534.720	474.870	59.850
8	584.233	510.917	73.316
9	722.185	645.876	76.309
10	875.940	789.158	86.782
11	1026.497	923.256	103.241
12	1096.616	987.390	109.226
13	1189.937	1060.827	129.110
14	1164.627	1078.183	86.444
15	1138.953	1095.539	43.414
16	1144.465	1104.218	40.247
17	1115.945	1086.861	29.084
18	809.579	878.995	69.416
19	846.955	798.198	48.757
20	825.091	709.880	115.211
21	755.625	650.888	104.737
22	712.835	611.090	101.745
23	644.520	557.737	86.783
24	562.240	490.420	71.820
Total	18885.940	17252.621	1633.319

Accordingly, the cost reduction is equal to 1633.319$ indicating the effect of the PVs on the cost reduction. Table IX tabulates the simulation results for the nonlinear problem. The total costs of without and with PVs are 19906.511$ and 19472.506$, respectively. As a result, the cost reduction is equal to 726.358$. The error percentages of the linearizing problem for no PV and with PV are 5.12 % and 11.4%, respectively. The execution time of the simulation is shown in Table X. For instance, the execution time in case I (no PV) for both linear and nonlinear problems are 1055 and 11394 seconds, respectively illustrating the effect of linearization on reducing the computational time.

Case II: Deterministic Problem: In this case, uncertainty and PVs are not considered. The results are shown in Table XI. As seen, with respect to previous case, the cost is increased by increasing the load. The total costs in LP and NLP are 15465.042$ and 16191.4$, respectively. The execution time of simulation is shown in Table XII. Computation time for the LP is 1036 seconds and in NLP is 10867 seconds. Same as the previous case, the linearization has reduced computational time.

TABLE IX: Hourly and total cost results for nonlinear problem (case I)

hour	Operation cost ($) (no PV)	Operation cost ($) (with PV)	Cost reduction($)
1	541.449	541.449	0
2	526.740	526.740	0
3	516.919	516.919	0
4	513.031	513.031	0
5	510.392	510.392	0
6	526.443	526.443	0
7	534.720	534.720	0
8	584.234	584.233	0

9	722.185	722.185	0
10	875.940	875.940	0
11	1026.498	1026.498	0
12	1096.616	1096.616	0
13	1197.278	1191.000	6.278
14	1252.967	1208.357	44.61
15	1311.958	1225.937	86.021
16	1327.788	1235.114	92.674
17	1311.205	1217.035	94.170
18	1080.354	1000.191	80.163
19	949.483	919.394	30.089
20	825.091	825.091	0
21	755.625	755.625	0
22	712.835	712.835	0
23	644.520	644.520	0
24	562.240	562.240	0
Total	19906.511	19472.506	434.005

TABLE X: Time duration of simulation (case I)

Type of problem	Linearized problem (no PV)	Linearized problem (PV included)	Nonlinear problem (no PV)	Nonlinear problem (PV included)
Computation time (s)	1055	1061	11394	11535

TABLE XI: Hourly and total costs (case II)

Hour	Operation cost ($) (linearized problem)	Operation cost ($) (nonlinear problem)	Difference ($)
1	445.000	445.000	0
2	445.000	445.000	0
3	445.000	445.000	0
4	445.000	445.000	0
5	445.000	445.000	0
6	445.000	445.000	0
7	445.000	445.000	0
8	445.000	445.000	0
9	547.000	547.000	0
10	677.000	677.000	0
11	790.000	790.000	0
12	846.500	846.500	0
13	860.236	958.000	97.764
14	974.882	1082.200	107.318
15	1017.347	1219.700	202.353
16	1035.819	1251.000	215.181
17	1127.258	1231.000	103.742
18	889.500	889.500	0
19	695.000	695.000	0
20	560.500	560.500	0
21	515.000	515.000	0
22	479.000	479.000	0
23	445.000	445.000	0
24	445.000	445.000	0
Total	15465.042	16191.400	726.358

TABLE XII: Time duration of simulation (case II)

Type of problem	Linearized problem	Nonlinear problem
Duration time (seconds)	1036	10867

C. Comparing LHSR with SP and RO

In this subsection, the simulation results on IEEE 69-bus are represented in Table XIII. In (3), if the ε is neglected, the proposed method is equivalent to SP and if the λ is ignored in (3), the proposed method is equivalent to RO. It is noted that the results in Table XIII are related to the linear problem (no PV).

TABLE XIII: Objective function in different methods

Type of method	LHSR	Deterministic	RO	SP
Cost ($)	18885.940	15465.042	19345.230	19674.560

As can be seen from the results, the cost of a RO and SP is greater than the proposed LHSR due to neglecting the parameters λ and ε.

VI. CONCLUSION

Within the context of day-ahead generation scheduling under load and PV uncertainties, an innovative framework approach has been proposed to deal with the aforementioned uncertainties. Numerical results of this paper on the IEEE 33-bus and 69-bus distribution test systems reveal the following conclusions:

- The linearized model reduces the execution time by about 90% while the difference between the results of the linear and nonlinear cases is low. Hence, the proposed model is effective because moderate computational burden within practical time frames has been necessary to achieve a high-quality near-optimal solutions.
- The proposed analytical method can replace the current practice in uncertainty modeling for the operation of distribution networks.
- The proposed model is useful to the system operator as the model including the uncertainty allows the simulation of possible realistic states of the system. Indeed, this issue helps in the necessity of the minimum changes in real practice of the operation decisions.

As the proposed probabilistic method is based on the assumption of Beta probability distribution of PVs, the future research may focus on extending the core models with other PDFs (i.e., Rayleigh, Weibull). The model can also be enriched by adding concepts like incorporating demand response programs to deal with the uncertainties of the RESs.

Appendix

The load profile and electricity price are given as follows:

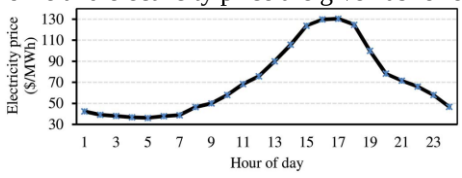

Day-ahead wholesale electricity prices for 33-bus [21]

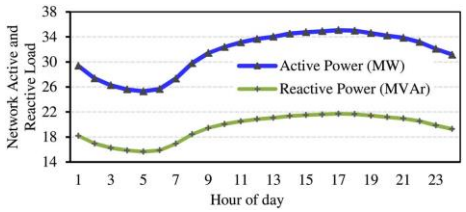

Forecasted day-ahead load profile of the AND for 33-bus [21]

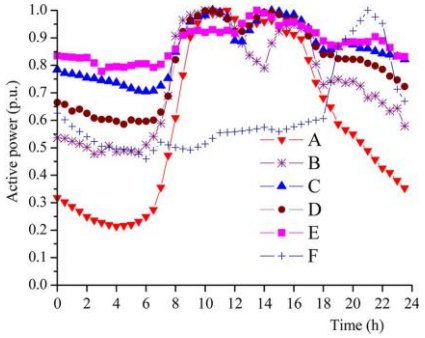

Typical daily load curves for 69-bus [23]

ACKNOWLEDGEMENT

This work is carried out as part of the InteGRIDy project. InteGRIDy project is being financed by the European Commission under Grant agreement 731268.

REFERENCES

[1] F. Luo, Z. Y. Dong, Z. Xu, W. Kong, and F. Wang, "Distributed residential energy resource scheduling with renewable uncertainties," *IET Generation, Transmission & Distribution*, vol. 12, no. 11, pp. 2770-2777, 2018.

[2] P. Chiradeja, "Benefit of distributed generation: A line loss reduction analysis," in *Transmission and Distribution Conference and Exhibition: Asia and Pacific, 2005 IEEE/PES*, 2005, pp. 1-5: IEEE.

[3] J. Aghaei, A. Nikoobakht, P. Siano, M. Nayeripour, A. Heidari, and M. Mardaneh, "Exploring the reliability effects on the short term AC security-constrained unit commitment: A stochastic evaluation," *Energy*, vol. 114, pp. 1016-1032, 2016.

[4] P. Rossoni, W. M. da Rosa, and E. A. Belati, "Linearized AC load flow applied to analysis in electric power systems," *IEEE Latin America Transactions*, vol. 14, no. 9, pp. 4048-4053, 2016.

[5] A. W. Bizuayehu, A. A. S. de la Nieta, J. Contreras, and J. P. Catalao, "Impacts of stochastic wind power and storage participation on economic dispatch in distribution systems," *IEEE Transactions on Sustainable Energy*, vol. 7, no. 3, pp. 1336-1345, 2016.

[6] H. Zhang, D. Yue, and X. Xie, "Robust optimization for dynamic economic dispatch under wind power uncertainty with different levels of uncertainty budget," *IEEE Access*, vol. 4, pp. 7633-7644, 2016.

[7] M. Asensio and J. Contreras, "Stochastic unit commitment in isolated systems with renewable penetration under CVaR assessment," *IEEE Transactions on Smart Grid*, vol. 7, no. 3, pp. 1356-1367, 2016.

[8] H. Hanhuawei *et al.*, "A two-stage stochastic programming method for optimal power scheduling with solar power integration," in *Chinese Automation Congress (CAC), 2017*, 2017, pp. 2041-2047: IEEE.

[9] A. Bhattacharya, J. P. Kharoufeh, and B. Zeng, "Managing energy storage in microgrids: A multistage stochastic programming approach," *IEEE Transactions on Smart Grid*, vol. 9, no. 1, pp. 483-496, 2018.

[10] T. Ding, C. Li, Y. Yang, J. Jiang, Z. Bie, and F. Blaabjerg, "A two-stage robust optimization for centralized-optimal dispatch of photovoltaic inverters in active distribution networks," *IEEE Transactions on Sustainable Energy*, vol. 8, no. 2, pp. 744-754, 2017.

[11] T. Ding, S. Liu, W. Yuan, Z. Bie, and B. Zeng, "A two-stage robust reactive power optimization considering uncertain wind power integration in active distribution networks," *IEEE Transactions on Sustainable Energy*, vol. 7, no. 1, pp. 301-311, 2016.

[12] X. Lin, S. L. Janak, and C. A. Floudas, "A new robust optimization approach for scheduling under uncertainty:: I. Bounded uncertainty," *Computers & chemical engineering*, vol. 28, no. 6-7, pp. 1069-1085, 2004.

[13] S. L. Janak, X. Lin, and C. A. Floudas, "A new robust optimization approach for scheduling under uncertainty: II. Uncertainty with known probability distribution," *Computers & chemical engineering*, vol. 31, no. 3, pp. 171-195, 2007.

[14] A. Nikoobakht, M. Mardaneh, J. aghaei, V. Guerrero-Mestre, J. Contreras, "Flexible power system operation accommodating uncertain wind power generation using transmission topology control: an improved linearised AC SCUC model," *IET Generation, Transmission & Distribution*, vol. 11, no. 1, pp. 142-153, 2017.

[15] A. Nikoobakht, J. Aghaei, M. Mardaneh. "Securing highly penetrated wind energy systems using linearized transmission switching mechanism," *Applied energy*, vol. 190, pp. 1207-1220, 2017.

[16] H. Cherif and J. Belhadj, "Energy output estimation of hybrid Wind-Photovoltaic power system using statistical distributions," *Journal of Electrical Systems*, vol. 10, no. 2, 2014.

[17 S. Trashchenkov and V. Astapov, "The applicability of zero inflated Beta distributions for stochastic modeling of PV plants' power output," in *2018 19th International Scientific Conference on Electric Power Engineering (EPE)*, 2018, pp. 1-6: IEEE.

[18] Y. Lv, L. Guan, Z. Tang, and Q. Zhao, "A Probability Model of PV for the Middle-term to Long-term Power System Analysis and Its Application," *Energy Procedia*, vol. 103, pp. 28-33, 2016.

[19] GAMS. The Solver Manuals. 1996 [Online]. Available: http://www.gams.com/.

[20] M. E. Baran and F. F. Wu, "Network reconfiguration in distribution systems for loss reduction and load balancing," *IEEE Transactions on Power delivery*, vol. 4, no. 2, pp. 1401-1407, 1989.

[21] S. Golshannavaz, S. Afsharnia, and F. Aminifar, "Smart distribution grid: optimal day-ahead scheduling with reconfigurable topology," *IEEE Transactions on Smart Grid*, vol. 5, no. 5, pp. 2402-2411, 2014.

[22] Output PV power [online]. Available: https://www.renewables.ninja.

[23] M. B. Liu, A. C. Canizares, W. Huang, "Reactive power and voltage control in distribution systems with limited switching operations," *IEEE Transactions on Power Systems*, vol. 24, no. 2, pp. 889-899, 2009.

[24] M. E. Baran, F. F. Wu, "Optimal capacitor placement on radial distribution systems," *IEEE Transactions on power Delivery*, vol. 4, no. 1, pp. 725-734, 1989.